CYP199A4 catalyses the efficient demethylation and demethenylation of *para*-substituted benzoic acid derivatives

Tom Coleman[1], Rebecca R. Chao[1], John B. Bruning[2], James J. De Voss[3] and Stephen G. Bell[1,*]

1 Department of Chemistry, University of Adelaide, SA, 5005, Australia; email: stephen.bell@adelaide.edu.au

2 Department of Molecular and Cellular Biology, University of Adelaide, Adelaide, SA, 5005, Australia.

3 School of Chemistry and Molecular Biosciences, University of Queensland, Brisbane, Qld, 4072, Australia

TOC

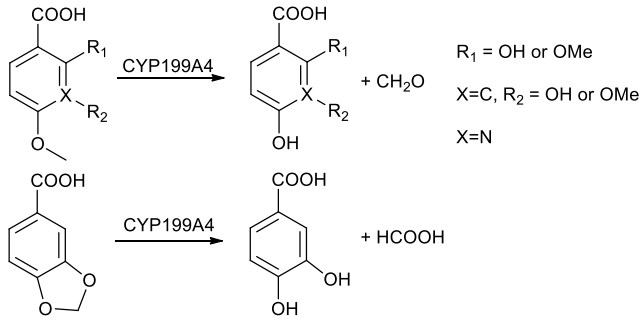

CYP199A4, a cytochrome P450 enzyme from *Rhodopseudomonas palustris* HaA2, is able to efficiently demethylate a range of benzoic acids at the *para*-position. It can also catalyse demethenylation reactions.

Abstract

The cytochrome P450 enzyme CYP199A4, from *Rhodopseudomonas palustris* strain HaA2, can efficiently demethylate 4-methoxybenzoic acid via hemiacetal formation and subsequent elimination of formaldehyde. Oxidative demethylation of a methoxy group *para* to the carboxyl moiety is strongly favoured over reaction at one in the *ortho* or *meta* positions. Dimethoxybenzoic acids containing a *para*-methoxy group were also efficiently demethylated exclusively at the *para* position. The presence of additional methoxy substituents reduces the substrate binding affinity and the activity compared to 4-methoxybenzoic acid. The addition of the smaller hydroxy group to the *ortho* or *meta* positions or of a nitrogen heteroatom in the aromatic ring of the 4-methoxybenzoate skeleton was better tolerated by the enzyme and these analogues were also readily demethylated. There was no evidence of methylenedioxy ring formation with 3-hydroxy-4-methoxybenzoic acid, an activity which is observed with certain plant CYP enzymes with analogous substrates. CYP199A4 is also able to deprotect the methylenedioxy group of 3,4-(methylenedioxy)benzoic acid to yield 3,4-dihydroxybenzoic acid and formic acid. This study defines the substrate range of CYP199A4 and reveals that substrates without a *para* substituent are not oxidised with any significant activity. Therefore *para*-substituted benzoic acids are ideal substrate scaffolds for the CYP199A4 enzyme and will aid in the design of optimised probes to investigate the mechanism of this class of enzymes. It also allows an assessment of the potential of CYP199A4 for synthetic biocatalytic processes involving selective oxidative demethylation or demethenylation.

Introduction

Cytochrome P450 (CYP) enzymes are heme-dependent monooxygenases with physiological roles that include hormone and secondary metabolite biosynthesis, as well as xenobiotic metabolism.[1-3] CYP enzymes primarily catalyse the insertion of an oxygen atom from dioxygen into carbon-hydrogen bonds of organic molecules. Mechanistically, hydrogen abstraction by Compound I is followed by oxygen rebound to give the hydroxylated compound.[4, 5] Many other types of activity are also known and include C–C bond cleavage and formation, oxidative dealkylation and various ring alterations.[2, 3, 6, 7] The stable, soluble nature of bacterial CYP enzymes and the wide range of compounds they oxidise are of interest for applications in synthesis involving C–H bond oxidation.[8, 9] The ability to engineer these bacterial CYP enzymes via rational or random methods can further enhance their activities and broaden their substrate range.[8, 10] A detailed knowledge of the enzyme-substrate interactions is critical in these efforts in order to maximise the catalytic efficiency of the CYP systems and to achieve the turnover numbers required for synthetic applications.

Rhodopseudomonas palustris is a family of purple photosynthetic bacteria that are isolated in temperate, aquatic sediments and possess extraordinary metabolic versatility. Bacteria classified as *Rhodopseudomonas* spp. can grow with or without light or oxygen, fix nitrogen and have a wide range of biodegradative abilities.[11] Studies have shown that different *Rhodopseudomonas* species share many characteristics but different strains have unique sets of functional genes to take advantage of the microenvironment in which they are found. We recently reported the properties of the complete CYP199A4 class I P450 system, from the *R. palustris* strain HaA2, which uses an electron transfer chain consisting of a [2Fe-2S] ferredoxin (HaPux) and a flavin-dependent ferredoxin reductase (HaPuR) to mediate heme reduction by NADH.[12-17] CYP199A4 and the closely related CYP199A2 enzyme, from *R. palustris* strain CGA009, have high affinities for 4-methoxybenzoic acid.[12, 13, 17] The

benzoic acid skeleton is important for binding and replacing it with a benzyl alcohol or a benzaldehyde reduces the strength of substrate binding dramatically.[12, 18] Altering the benzene ring to a saturated cyclohexyl system or removal of the substituent at the *para*-position both have a deleterious effect on substrate binding and activity.[12, 18]

In addition to 4-methoxybenzoic acid, CYP199A4 can bind and *O*-demethylate 3,4-dimethoxybenzoic acid (veratric acid) solely at the 4-methoxy group to yield 3-methoxy-4-hydroxybenzoic acid (vanillic acid). However the spin state shift observed upon substrate binding is reduced, the binding is not as tight and the activity is lower.[17] CYP199 enzymes have also been reported to be biocatalysts for the oxyfunctionalisation of various aromatic carboxylic acids including 2-naphthoic acid, indole-6-carboxylic acid and cinnamic acids.[19-21] Recently mutant forms of the CYP199A2 enzyme have been shown to catalyse the oxidation of benzyl alcohols and phenols using a whole-cell oxidation system. However detailed analysis of the substrate-enzyme interactions were not presented.[22]

The crystal structure of substrate-free and 4-methoxybenzoic acid-bound forms of CYP199A4 have been determined (PDB: 4DNZ and 4DO1).[13, 18, 23] In the substrate-bound structures the substrate carboxylate group interacts with polar and basic amino acid side chains while hydrophobic interactions with the benzene ring help hold the substrate in position. These interactions account for the efficiency and substrate specificity of the enzyme. In the crystal structure of 4-methoxybenzoic acid-bound CYP199A4, the substrate carboxylate group forms hydrogen bonds directly to the side chains of Arg92, Ser95 and Ser244 and, via a bridging water molecule, Arg243. The addition of the substrate triggers movement in these residues and is accompanied by the binding of a chloride ion.[23] These structural changes cap the entrance to the active site and protect the heme from the external solvent. The methyl group of the *para*-methoxy substituent is oriented towards the heme iron (3.9 Å), which is consistent with exclusive attack at this position, leading to demethylation to

form 4-hydroxybenzoic acid. The crystal structure of CYP199A4 with 3,4-dimethoxybenzoic acid (PDB: 4EGN) reveals that the introduction of a methoxy group at the *meta* position causes steric clashes with active site residues, Phe182 and Phe185, which presumably leads to the reduced efficiency of binding and therefore activity.[18]

The chemical removal of methyl protecting groups often requires harsh conditions and unselective reagents.[24] Alkyl methyl ethers usually require a Lewis acid and a nucleophile for efficient demethylation while aryl methyl ethers, such as 4-methoxybenzoic acid, can be demethylated in the absence of the Lewis acid. However the CYP enzyme-catalysed *O*-demethylation reaction proceeds under ambient conditions. CYP enzymes are attractive targets for carrying out selective oxidative demethylation and therefore the deprotection of methoxy groups under mild conditions.

Here we compare the binding and kinetic properties of CYP199A4 with selected substituted methoxybenzoic acid substrates. These studies will provide a basis for understanding how benzoic acids with differently sized substituents at the *ortho*- and *meta*-positions or a heteroatom in the benzene ring interact with and are oxidized by the enzyme. We also investigate if CYP199A4 is able to catalyse the demethenylation of 3,4-(methylenedioxy)benzoic acid. This will provide a basis for the future synthesis of small molecule probes designed to investigate the subtleties of the mechanism of action of CYP enzymes as well as the design of better biocatalysts using this system.

Results and discussion

Substrate binding studies on the CYP199A4 system

We had shown previously that binding of 4-methoxybenzoic acid to CYP199A4 induces a ≥ 95% Type I spin state shift (Table 1) while 3,4-dimethoxybenzoic acid (veratric acid) only shifts the spin state to 70% high-spin.[17] Binding of 3,4-dimethoxybenzoic acid to CYP199A4 was also two orders of magnitude (29.5 μM) weaker compared to 4-methoxybenzoic acid (0.28 μM). A comparison of the crystal structures of substrate-bound forms of CYP199A4 with these two substrates reveals that the phenyl rings, the carboxylate group and 4-methoxy substituent are, to all practical purposes, superimposable. The 3-methoxy substituent of 3,4-dimethoxybenzoic acid points away from the heme and it makes contact with the benzene ring of Phe182 and Phe185. This causes Phe182 to move, resulting in changes in the location of the side chains of Leu396 and Asp251. These steric clashes presumably are the main contributing factor to the weaker binding of this substrate and the relative location of the two methoxy groups to the heme iron provides a compelling rationale for demethylation only at the *para* substituent. In this work a range of substituted benzoic acid derivatives was tested to further probe the limits of substrate shape and electronic structure on CYP199A4 substrate binding and activity (Fig. 1a).

2-Methoxy- and 3-methoxybenzoic acid both induced a significantly lower spin state shift to the high-spin form than 4-methoxybenzoic acid, with the 3-methoxy variant giving a greater shift than the 2-methoxy isomer (Table 1, Fig. 1b and Fig. S1). Benzoic acid bound to CYP199A4 and induced a spin state shift of 30% which is higher than that induced by 2-methoxybenzoic acid but lower than those of 3- and 4-methooxybenzoic acids. Dimethoxybenzoic acids which lack the substituent at the *para*-position also induced minimal spin state shifts in CYP199A4, though that of 3,5-dimethoxybenzoic acid was higher than that of 2,5-dimethoxybenzoic acid (Table 1 and Fig. S1). This highlights that the *para*-

methoxy substituent, or equivalent, is a requirement for removal of the water bound to the heme iron when substrate binds. This agrees with previous data obtained for CYP199A2 where the addition of benzoic acid induces a lower shift than 4-methoxybenzoic acid and both 2-chlorobenzoic acid and 3-chlorobenzoic acid bind poorly compared to 4-chlorobenzoic acid.[12] The *para*-methoxy group of 4-methoxybenzoic acid interacts with Phe182 and Phe298 and is held over the heme in an ideal position for C–H bond abstraction.[23] These interactions could stabilise the binding of this substrate over benzoic acid alone. The lack of the *para*-methoxy group and the presence of groups at the *ortho*- or *meta*-positions, which could result in steric clashes with active site amino acids or the heme, reduce the binding affinity of these benzoic acids. Benzoic acids which only contain a substituent at the *para*-position may also have more freedom to rotate in the substrate binding pocket of CYP199A4 resulting in more favourable binding. As the presence of a substituent *para* to the carboxylic acid was found to be important for substrate binding we decided to explore the effect of additional substituents at the *ortho*- and *meta*-positions. Therefore we studied the binding of differently substituted 4-methoxybenzoic acids (Fig. 1a).

2,4-Dimethoxy-, 2-hydroxy-4-methoxy and 3-hydroxy-4-methoxy-benzoic acids induced a spin state shift of ≥ 90%, all of which are greater than that observed with 3,4-dimethoxybenzoic acid (Table 1, Fig. 1 and Fig. S1). 3-Hydroxy-4-methoxy benzoic acid with the smaller hydroxy group at the *meta*-position appears to be better accommodated in the substrate binding pocket than 3,4-dimethoxybenzoic acid which has a larger methoxy moiety at the analogous position. In addition, having the methoxy group *ortho* to the carboxylate group, as in 2,4-dimethoxybenzoic acid, appears not to disrupt binding as much as the 3,4-dimethoxybenzoic acid. We also investigated the effect of inserting a heteroatom at the *meta*-position of the benzene ring. 6-Methoxynicotinic acid induced a ≥ 95% type I spin state shift (Fig. S1), indicating that a nitrogen-containing aromatic ring does not dramatically

affect substrate binding. These substrates may be orientated with the nitrogen, hydroxy or methoxy moiety either directed towards the heme ring or pointing at the Phe182 and Phe185 residues (or in a mixture of both orientations). However the large spin state shift infers the nitrogen or the hydroxy substituents do not interfere with the dissociation of the 6th water ligand in whichever orientation it is bound.

The size of the substrate and the nature of the substitutions which can bind in the active site of CYP199A4 were further tested by investigating 3,4-(methylenedioxy)benzoic acid, which is structurally related to both 3,4-dimethoxybenzoic acid and 3-hydroxy-4-methoxybenzoic acid. This substrate induces a shift to 70% high-spin which is comparable to that observed with the larger 3,4-dimethoxybenzoic acid but lower than that observed with 3-hydroxy-4-methoxybenzoic acid (Table 1 and Fig. 1). The methylenedioxy group may be held with the methylene group located in a similar position to the methyl of the *para*-methoxy substituent of 3,4-dimethoxybenzoic acid where the 3-methoxy group points away from the heme and towards Phe182 as revealed in the crystal structure of 3,4-dimethoxybenzoic acid–bound CYP199A4 (PDB: 4EGN); this could be the reason for the reduced spin state shift.[18] Alternatively, the methylenedioxy five membered ring may be orientated towards the heme in a similar position to that of the pyrole ring of indole-6-carboxylic acid-bound CYP199A4 (PDB: EGO, binding of this substrate induces a 20% shift to the high-spin form).[18]

While the spin state shift gives an indication of substrate binding neatly in the substrate binding pocket it does not provide detailed information on how tightly the substrate may be bound. To further analyse substrate binding, the dissociation constant (K_d) was determined for each substrate using UV-Vis titration experiments (Table 1, Fig. 2 and S2). 6-Methoxynicotinic acid binds tightly to CYP199A4 (K_d = 0.46 μM), highlighting that the heterocyclic ring does not significantly impair binding. 3-Hydroxy-4-methoxybenzoic acid

bound less tightly (K_d = 1.7 μM) than 4-methoxybenzoic acid and 6-methoxynicotinic acid but more tightly than 3,4-dimethoxybenzoic acid, confirming that the smaller hydroxyl group at this position is better accommodated in the active site of CYP199A4. 2-Hydroxy-4-methoxybenzoic acid bound as tightly as 4-methoxybenzoic acid. Despite the higher spin state shift observed on substrate binding, 2,4-dimethoxybenzoic acid bound more weakly than 3,4-dimethoxybenzoic acid and the larger methoxy substituent at the *ortho*-position must also impair substrate binding though not dissociation of the water ligand from the heme iron (Table 1 and Fig. 2). The most likely cause of the reduced binding affinity is steric clashes with amino acids in the active site of CYP199A4.

3,4-(Methylenedioxy)benzoic acid bound more tightly than both 3,4-dimethoxybenzoic acid and 3-hydroxy-4-methoxybenzoic acid suggesting improved interactions with the substrate binding pocket despite the lower spin state shift observed (Table 1 and Fig. S2). This may be due to combination of the more hydrophobic methylenedioxy ring, compared to the hydroxyl group in 3-hydroxy-4-methoxybenzoic acid, and the smaller size of the substrate compared to 3,4-dimethoxybenzoic acid. 3-Methoxybenzoic acid bound less tightly to CYP199A4 than any of the substrates which contain a methoxy group at the *para*-position (Table 1). 3-Methoxybenzoic acid bound to CYP199A4 two orders of magnitude more weakly than 4-methoxybenzoic acid and, despite its higher spin state shift, less tightly than benzoic acid suggesting the 3-methoxy group interacts less favourably with the substrate binding pocket. The binding of 3,5-dimethoxybenzoic acid was 20-fold weaker than 3-methoxybenzoic acid in line with the low spin state shift observed. The negligible spin state shifts induced by the 2-methoxybenzoic and 2,5-dimethoxybenzoic acids prevented the accurate determination of the dissociation constant (K_d > 1.5 mM).

Overall the data indicates that a substituent *para* to the carboxylate moiety is beneficial for substrate binding and that additional, preferably smaller, substituents can be accommodated at the *ortho*- and *meta*-positions.

Activity and product formation assays

The rates of NADH oxidation and product formation varied considerably across the range of benzoic acid substrates though all were lower in activity when compared to 4-methoxybenzoic acid (Table 1 and Fig. 3).[17, 18] CYP199A4 had no observable NADH oxidation or product formation activity with 2-methoxybenzoic and 2,5-dimethoxybenzoic acids (Fig. S3a and b). CYP199A4 in the presence of 3-methoxybenzoic acid did oxidise NADH but no product from substrate oxidation could be detected via HPLC or GC-MS analysis (Fig. S3c) and similar results were obtained for benzoic acid (Fig. S3). Furthermore very little hydrogen peroxide was generated in these turnovers. The percentage of reducing NADH equivalents channelled into hydrogen peroxide formation was 2.2 ± 0.7% for 3-methoxybenzoic acid and 4.7 ± 0.3% for benzoic acid (Table 1) suggesting the elevated NADH oxidation rate is most likely due to the oxidase uncoupling pathway. This presumably arises as the 3-methoxy substituent or any other C–H bond is not close enough to the reactive iron-oxo intermediate to be oxidised.[25, 26] Of the substrates which lack a 4-methoxybenzoic acid moiety only 3,5-dimethoxybenzoic acid yielded any observable product. However the rate of NADH oxidation is very slow and the levels of product formation are extremely low with a single product being observed by HPLC (Table 1 and Fig. 4a). In the absence of an authentic product standard the turnover was derivatised with BSTFA/TMSCl and analysed by GC-MS (Fig. 5a). The product has a mass of 312.1 AMU which corresponds to a doubly TMS-derivatised species arising from a single oxidative demethylation of the substrate to yield 3-hydroxy-5-methoxybenzoic acid (Scheme 1 and Fig. S4a). The observation of even a small amount of product with 3,5-dimethoxybenzoic acid is interesting as the related 3-

methoxybenzoic acid is not oxidatively demethylated by CYP199A4 and this information when combined with the significantly different spin state shift on substrate binding suggests a different binding mode for these two molecules in the active site.

In the CYP199A4 substrate-bound crystal structures with 4-methoxybenzoic, 4-ethylbenzoic and 3,4-dimethoxybenzoic acids, (PDB codes: 4DO1, 4EGM and 4EGN, respectively) the benzoic acid components of the substrates are superimposed. The substituent in the *para* position is held over the heme iron for efficient oxidation while the 3-methoxy substituent of 3,4-dimethoxybenzoic acid points away from the heme towards Phe182. Given that substrates which do not have a 4-methoxy substituent give rise to low levels of product formation it is likely that the other substituents, such as a 3-methoxy group, point away from the heme. In the case of 3,5-dimethoxybenzoic acid if one methoxy group points at Phe182 the other must be orientated towards the heme. Despite not sterically displacing the iron-bound water molecule and modifying the spin state, it is close enough to result in low levels of a single demethylated product. 3,5-Dimethoxybenzoic acid was docked into the substrate binding pocket of 4-methoxybenzoic acid-bound CYP199A4 (PDB: 4DO1), minus the substrate, and energy minimised. Compared to the structure of 3,4-dimethoxybenzoic acid and other analogues the benzoic acid moiety was tilted by 15 ° (Fig. 6a). In this position the 3-methoxy methyl carbon is only 5.0 Å from the heme iron (the oxygen of the same methoxy group is 0.2 Å closer). The 3-methoxy carbon is also 2.8 Å from both Leu98, and the closest heme carbon atom and 3.0 Å from a heme nitrogen. The 5-methoxy group points towards Phe182 with both the oxygen and methyl carbon being 2.9 Å from the closest atom of this residue (Fig. 6a). This altered binding orientation may explain the observation of an oxidative demethylation product, in contrast to 3-methoxybenzoic acid, while the long Fe-C (O-Me) distance gives rise to the reduced product formation rate, which is two orders of magnitude lower, compared to 4-methoxybenzoic acid (Fig. 6a). The altered

binding orientation of 3,5-dimethoxybenzoic acid is much less favourable, resulting in a 20-fold decrease in binding and a 5000-fold decrease in activity relative to 4-methoxybenzoic acid.

The oxidation of all the remaining substrates by CYP199A4 resulted in the formation of a single product arising through demethylation of a methoxy group at the *para*-position, or in the case of 3,4-(methylenedioxy)benzoic acid, demethenylation of the methylenedioxy group (Scheme 1). The products were identified via co-elution of authentic standards via HPLC or GC-MS analysis of the trimethylsilyl derivatives (Fig. 4, and S3). Levels of product formation were determined using HPLC or GC-MS after calibrating with the product standards.

The CYP199A4 catalysed turnover of 6-methoxynicotinic acid displayed a NADH oxidation rate of 353 nmol (nmol-CYP)$^{-1}$ min^{-1} (Table 1 and Fig. 3), which demonstrates the pyridine heterocyclic ring has a detrimental effect on the enzyme's activity despite the substrate binding data indicating that 6-methoxynicotonic acid can bind effectively to the CYP199A4 enzyme. The product was confirmed as arising from oxidative demethylation via co-elution of the turnover with an authentic sample of 6-hydroxynicotinic acid with the turnover mixture via HPLC (Fig. 4b). GC-MS analysis of the BSTFA/TMSCl-derivatised turnover mixture yielded product of the predicted mass (*m/z* of 283.2 AMU *vs*. the expected *m/z* of 283.1 AMU). There was no evidence of N-oxide formation via GC-MS or HPLC. The product formation rate was 286 nmol (nmol-CYP)$^{-1}$ min^{-1} indicating that the coupling of NADH reducing equivalents to product formation was high (81%). Therefore the four-fold lower activity of the 6-methoxynicotinic acid compared to 4-methoxybenzoic acid is due to slower turnover rate of the catalytic cycle. The incorporation of a nitrogen atom *meta* to the carboxylate group in the aromatic ring (*ortho* to the methoxy group) results in a lower activity. This nitrogen contains a non-bonded lone pair which is not part of the aromatic ring

and the nitrogen is considered to be electron withdrawing. The substrate may be orientated with the nitrogen either directed towards the heme ring or pointing at the Phe182 and Phe185 residues. If it was directed towards the heme iron it would be expected to be a similar distance from the iron as the C3 carbon of 4-methoxybenzoic acid (5.1 Å). Docking of the 6-methoxynicotinic acid substrate in the CYP199A4 active site with the nitrogen in this position, followed by energy minimisation, resulted in a structure where this nitrogen was only 5.2 Å from the heme iron (Fig. 5b). This compares to the 6-methoxy carbon which is only 3.9 Å away. If the nitrogen is directed towards the heme it could interfere with the formation or cleavage of heme iron-oxygen adducts. We note the lack of any N-oxide formation which would be evidence of the substrate being orientated with the nitrogen closer the heme. However we cannot yet rule out an altered substrate binding orientation. The N-containing heterocycle is less sterically hindered than a *meta* substituted benzene ring and therefore 6-alkyl substituted nicotinic acid derivatives could be useful probes to further investigate the partition between desaturation and hydroxylation of alkyl side chains by CYP199A4 using the electron withdrawing pyridine ring.

2,4-Dimethoxybenzoic acid is efficiently turned over to yield one product which was confirmed by GC-MS to correspond to a single demethylation (Fig. 5b and S3d). Based on all the previous data obtained for substituted 4-methoxybenzoic acids with CYP199A4 it is likely that the product is a result of oxidative demethylation *para* to the carboxyl group to yield 2-methoxy-4-hydroxybenzoic acid (Fig. S5). The turnover activity and coupling of 2,4-dimethoxybenzoic acid with CYP199A4 were lower than 3,4-dimethoxybenzoic acid. Both 2- and 3-hydroxy-4-methoxybenzoic acids were turned over by CYP199A4 generating a single product (2,4- and 3,4-dihydroxybenzoic acids, respectively, Fig. 4c and Fig. S3e). The product formation rate of the 3-hydroxy analogue was higher than that of 2-hydroxy-4-methoxybenzoic acid (Table 1). This is in line with the NADH oxidation activities but not the

tighter binding of the 2-hydroxy analogue. The activity and coupling of the substrates with a hydroxyl or methoxy substituent at the 3-position were higher than those with the equivalent substitutions at the 2-position (Table 1).

Certain plant P450 enzymes, such as CYP719A can catalyse the oxidative cyclisation of *ortho*-hydroxymethoxy-containing substrates resulting in the formation of a methylenedioxy ring. This reaction is important, for example, in isoquinoline alkaloid biosynthesis.[27, 28] There was no evidence for the formation of a methylenedioxy bridge in the CYP199A4 catalysed turnover of 3-hydroxy-4-methoxybenzoic acid. Methylenedioxy-bridge formation is proposed to occur in the plant enzymes by P450-dependent hydroxylation of the methoxy group yielding a hemiacetal which cyclises to form the methylenedioxy bridge by an ionic mechanism, involving a methylene oxonium ion intermediate (Scheme 2). The evidence for this mechanism is that no oxygen is incorporated into the product. The hemiacetal precursor to ring formation is the same as that which would be generated in the oxidative demethylation reaction of 3-hydroxy-4-methoxybenzoic acid. In CYP199A4 3-hydroxy-4-methoxybenzoic acid may be bound in a similar fashion to 3,4-dimethoxybenzoic acid with the substituent in the 3-position pointing away from the heme iron (Fig. S5). In this orientation the methyl of the 4-methoxy group points towards the heme iron and away from the 3-hydroxy group allowing rapid hemiacetal formation and demethylation rather than methylenedioxy ring formation. If the hydroxy group points towards the heme it is located only 4.3 Å from the iron. The plant P450 enzymes, which carry out this transformation, must bind their substrates in such a way relative to the heme iron-oxo intermediate which favours this reaction over oxidative demethylation or convert the intermediate radical directly to the cationic methylene oxonium ion.

As a substrate 3,4-(methylenedioxy)benzoic acid generates a single monooxygenase product, 3,4-dihydroxybenzoic acid (Fig. 4d). The demethenylation reaction proceeds with

lower activity than the demethylation of 4-methoxybenzoic acid, 3,4-dimethoxybenzoic acid and 3-hydroxy-4-methoxybenzoic acid. This would be unexpected if hydrogen abstraction was the rate determining step due to the favourable electronic effect of two oxygen atoms. The substrate must be held in the substrate binding pocket with the methylene C-H bonds located in a less favourable position for attack by compound I compared to the methyl moieties of the methoxy groups of the other substrates. This may be due to the constrained nature of the five membered ring resulting in the methylene group being bound further away from the heme iron. Docking of 3,4-(methylenedioxy)benzoic acid into the substrate binding pocket followed by energy minimisation indicated it could bind in a similar orientation to indole-6-carboxylic acid (PDB: EGO) which places the methylenedioxy bridge only 4.0 Å from the heme iron (Fig. 6c), compared to 3.8 Å for the methoxy carbon of 4-methoxybenzoic acid (PDB: 4DO1). However the substrate could also bind in a similar fashion to 3,4-dimethoxybenzoic acid (PDB: 4EGN) which would place the methylene carbon 5.7 Å away from the heme iron (Fig. 6c and Fig. S5).

Demethenylation is thought to occur by a three-step process involving initial oxidation of the methylene carbon, followed by a rearrangement and hydrolysis generating formic acid rather than formaldehyde, which is produced in oxidative demethylation (Scheme 3). To confirm this we analysed the turnovers of 3,4-methylenedioxy benzoic acid and 4-methoxybenzoic acid derivatives for the presence of formaldehyde and formic acid. The turnovers of 4-methoxybenzoic, 3,4-dimethoxybenzoic and 3-hydroxy-4-methoxybenzoic acids generated formaldehyde, as measured by the Purpald assay, in line with the levels of product observed (Fig. 7 and Fig. S6). Nugatory levels of formic acid were observed in these assays (formate assay, Megazyme). The turnover of 3,4-(methylenedioxy)benzoic acid showed the opposite results with low levels of formaldehyde but significant quantities of formic acid being produced in agreement with the mechanism proposed. To confirm the

absence of 3,4-(methylenedioxy)benzoic acid in the turnover of 3-hydroxy-4-methoxybenzoic acid, which may have been further oxidised to 3,4-dihydroxybenzoic acid, we also analysed this turnover reaction for the generation of formic acid as well as formaldehyde. Only formaldehyde was found to be present and the lack of any formic acid rules out further processing of any generated methylenedioxy compounds during CYP199A4 mediated turnover of 3-hydroxy-4-methoxybenzoic acid.

Kinetic isotope studies on the reaction of mammalian P450s on methylenedioxy containing drug molecules have led to the proposal that an alternative pathway driven by peroxide based chemistry may compete with the mechanism outlined (Scheme 3).[29] The levels of uncoupling in the CYP199A4 catalysed reaction are relatively low therefore CYP199A4 could be used to study the mechanism of demethenylation in more detail. In addition there was no evidence of inhibition of turnover rates after initial oxidation of the methylenedioxy group (Fig. 4) as has been observed in the CYP2A6 metabolism of paroxetine which is proposed to be due to binding of a carbene species to the heme iron (Scheme 3 and Fig. 3).[30]

Overall we have shown that CYP199A4 catalyses the efficient oxidative demethylation of a range of *para*-substituted benzoic acid derivatives with concomitant formation of formaldehyde. Substituents of moderate size at the *ortho*- and *meta*-positions can be tolerated and oxidative demethenylation, which generates a diol and formic acid, is also catalysed efficiently by this enzyme. The binding of the benzoic acid substrates in CYP199A4 must be very tightly controlled as oxidation only occurs on the *para* substituent. With other P450s blocking the position of the closest C–H bonds, where hydroxylation is preferred, often leads to oxidation at another position often at an adjacent carbon.[31, 32] This makes CYP199A4 and *para* substituted benzoic acids an ideal enzyme-substrate combinations to ensure that only the desired functional groups is oxidised. This could be

utilised for selective demethylation or hydroxylation reactions on multiply substituted substrates. This also makes *para* substituted benzoic acids ideal substrate scaffolds with which to study different aspects of cytochrome P450 mechanism.

Experimental Section

General

General reagents, organic substrates and *N*,*O*-bis(trimethylsilyl)trifluoroacetamide with trimethylchlorosilane (BSTFA/TMSCl, 99:1) were from Sigma-Aldrich, TCI or Merck, Australia. Buffer components, NADH and isopropyl-β-D-thiogalactopyranoside (IPTG) were from Astral Scientific, Australia. UV/Vis spectra and spectroscopic activity assays were recorded at 30 ± 0.5 °C on an Agilent CARY-60 or Varian CARY-5000 spectrophotometer.

Enzymes and molecular biology

General DNA and microbiological experiments were carried out by standard methods.[33] The expression and purification of CYP199A4, HaPux, and HaPuR have been described elsewhere.[14, 17, 34] Proteins were stored at –20 °C in 50 mM Tris, pH 7.4 containing 50% v/v glycerol. Glycerol was removed immediately before use by gel filtration on a 5-mL PD-10 column (GE Healthcare, UK) by eluting with 50 mM Tris, pH 7.4. The CYP199A4 protein concentration was calculated using ε_{419} = 119 $mM^{-1}cm^{-1}$.[17, 23]

Activity assays

In vitro NADH turnover rate assays were performed with mixtures (1.2 mL) containing 50 mM Tris, pH 7.4, 0.5 μM CYP199A4, 5 μM HaPux, 0.5 μM HaPuR and 100 μg mL^{-1} bovine liver catalase. The buffer solution was oxygenated before use and the mixture equilibrated at 30 °C for 2 min. Substrates were added from a 100 mM stock solution in ethanol to a final concentration of 1 mM. NADH was added to *ca*. 320 μM (final A_{340} = 2.00) and the absorbance at 340 nm was monitored. The rate of NADH oxidation was calculated using ε_{340} = 6.22 $mM^{-1}cm^{-1}$.

Substrate binding: spin state determination and binding titrations

The high-spin heme content was estimated (to approximately ±5%) by comparison with a set of spectra generated from the sum of the appropriate percentages of the spectra of the

substrate-free (>95% low-spin, Soret maximum at 418 nm) and camphor-bound (>95% high-spin, Soret maximum at 392 nm) forms of WT CYP101A1.

For dissociation constant determination CYP199A4 was diluted to 0.5 – 2.0 μM using 50 mM Tris, pH 7.4, in 2.5 mL and 0.5 – 2 μL aliquots of the substrate were added using a Hamilton syringe from 1, 10 or 100 mM stock solutions in ethanol. The maximum peak-to-trough difference (ΔA) in absorbance between 700 nm and 250 nm was recorded. Further aliquots of substrate were added until the peak-to-trough difference did not change. The dissociation constants, K_d, were obtained by fitting ΔA against total substrate concentration [S] to a hyperbolic function:

$$\Delta A = \frac{\Delta A_{max} \times [S]}{K_d + [S]}$$

where ΔA_{max} is the maximum absorbance difference. Several substrates exhibited tight binding, with K_d < 2 μM. In these instances the data were fitted to the tight binding quadratic equation:[35]

$$\frac{\Delta A}{\Delta A_{max}} = \frac{([E]+[S]+K_d) - \sqrt{\{([E]+[S]+K_d)^2 - 4[E][S]\}}}{2[E]}$$

where ΔA_{max} is the maximum absorbance difference and [E] is the enzyme concentration.

Analysis of metabolites

After the NADH had been consumed in substrate oxidation incubations, 132 μL of the reaction mixture was mixed with 2 μL of an internal standard solution (10 mM 9-hydroxyfluorene in ethanol). This was mixed with 66 μL of acetonitrile before analysis by HPLC. Reverse phase HPLC was performed using an Agilent 1260 Infinity pump equipped with an Agilent Eclipse Plus C18 column (250 mm x 4.6 mm, 5 μm) and an autoinjector and UV detector. A gradient, 20 - 95%, of acetonitrile in water (both containing trifluoroacetic acid, 0.1%) was used and the absorbance was monitored at 254 nm (unless otherwise stated).

The retention times for the substrates and products were as follows; 2-methoxybenzoic acid, 11.9 min; 3-methoxybenzoic acid, 13.0 min; 4-methoxybenzoic acid, 12.5 min; 4-hydroxybenzoic acid, 6.8 min; 3-hydroxybenzoic acid, 8.2 min; 6-methoxynicotinic acid, 7.0 min; 6-hydroxynicotinic acid, 5.1 min; 2-hydroxy-4-methoxybenzoic acid, 13.9 min; 2,4-dihydroxybenzoic acid, 8.5 min; 3-hydroxy-4-methoxybenzoic acid, 7.9 min; 3,4-dihydroxybenzoic acid, 5.3 min; 3,4-(methylenedioxy)benzoic acid, 12.2 min; 3,4-dimethoxybenzoic acid, 12.0 min; 3-methoxy-4-hydroxybenzoic acid, 7.5 min; 2-methoxy-4-hydroxybenzoic acid, 7.4 min; 2,4-dimethoxybenzoic acid 11.9 min; 3,5-dimethoxybenzoic acid 13.8 min; 3-hydroxy-5-methoxybenzoic acid 9.9 min; 2,5-dimethoxybenzoic acid, 13.7 min.

For gas chromatography analysis 990 μL of the reaction mixture was mixed with 10 μL of an internal standard solution (10 mM 9-hydroxyfluorene in ethanol) and 2 μL of concentrated HCl. The mixture was extracted three times with 400 μL of ethyl acetate and the organic extracts were combined and dried over $MgSO_4$. Solvent was evaporated under a stream of dinitrogen and the sample dissolved in 200 μL acetonitrile. Excess (25 μL) BSTFA + TMSCl (99:1) was added and the mixture left for at least 120 min to produce the trimethylsilyl ester of the carboxylic acid group and trimethylsilyl ether of the alcohol, if formed. The resultant mixtures were used directly for GC analysis. The oven temperature was held at 120 ºC for 3 min and then increased at 10 ºC min^{-1} up to 220 ºC before being held for a further 7 min. The retention times for the trimethylsilyl (TMS) derivatised substrates and products were as follows; 4-methoxybenzoic acid, 7.8 min; 4-hydroxybenzoic acid, 11.2 min; 6-methoxynicotinic acid, 7.8 min; 6-hydroxynicotinic acid, 10.2 min; 2,4-dimethoxybenzoic acid, 14.2 min; 2-hydroxy-4-methoxybenzoic acid, 16.1 min; 3,5-dimethoxybenzoic acid, 13.7 min; 3-hydroxy-5-methoxybenzoic acid, 15.2 min.

Products were calibrated against authentic product standards where available. When authentic samples were not available the coupling was estimated based on the closest available compound from those above. For example for 2-methoxy-4-hydroxybenzoic acid, for which no authentic standard was available, the product peaks were calibrated against both the substrate (2,4-dimethoxybenzoic acid) and 2,4-dihydroxybenzoic acid to determine the HPLC detector response (the responses of both were very similar). These were then used to estimate the concentration of the product peak.

Formaldehyde, formic acid and hydrogen peroxide assays

The formaldehyde content of turnovers was determined using mixtures (600 µL) containing Tris buffer, pH 7.4, 50 mM (312 µL), the turnover mixture (240 µL) and Purpald (48 µL from 168 mM stock in 2M NaOH). The reaction of formaldehyde and Purpald was allowed to develop with shaking for 15 min before quantifying the formaldehyde Purpald complex (Scheme S1) using the absorbance at 550 nm and subsequent comparison to a calibration curve (Fig. S6).[36]

The formic acid content was determined using a formic acid assay kit from Megazyme. The turnover (1.1 mL), H_2O (1.0 mL), phosphate buffer (pH 7.6, 0.2 mL) and β-NAD (0.2 mL) were combined and equilibrated for 5 min. The absorbance at 340 nm was measured and formate dehydrogenase (50 µL) was added to consume formic acid and form NADH; this was allowed to react for 15 min. The increase in absorbance at 340 nm was used to quantify the formic acid. The concentration of hydrogen peroxide formed by uncoupling during NADH oxidation was determined by the horseradish peroxidase/phenol/4-aminoantipyrine assay as described previously.[37]

Docking Studies

Ligand coordinates and restraints were created using PHENIX eLBOW (PMID: 19770504). Ligands were initially docked manually into the active site of CYP199A4 (PDB: 4DO1), with

the 4-methoxybenzoic acid removed, using Coot (PMID: 20383002). Each model was individually subjected to regularization and model refinement with ICM-Pro (to carry out energy minimization, optimize model geometry, and alleviate clashing side chains). The protein-ligand complexes were subjected to 300 rounds of Cartesian MMFF energy minimization using ICM Pro (Molsoft, LLC). Side chains were globally optimized and the backbone was annealed to improve the model using the ICM Pro Monte Carlo algorithm.[38]

Conclusions

The substrate range of CYP199A4 has been assessed using a range of methoxybenzoic acid derivatives. A methoxy group at the *para* position is essential for optimal activity. Substitutions at other positions or the insertion of a heteroatom in the ring can be tolerated but the activity is reduced. CYP199A4 does not catalyse methylenedioxy ring formation with 3-hydroxy-4-methoxybenzoic acid but does catalyse oxidative demethenylation of 3,4-(methylenedioxy)benzoic acid. As a result the biocatalytic scope of CYP199A4 has been determined and this knowledge can be used to improve substrate binding and turnover of CYP199A4 with non-natural substrates through protein engineering. Probes which complement the size and shape of the substrate binding pocket of CYP199A4 can also be designed. This will minimise competing uncoupling pathways and allow the tight control the site on the probe which is attacked by the enzyme.

Acknowledgment

This work was supported by ARC grant DP140103229 (to JJDV and SGB). The authors also acknowledge the award of an Australian Postgraduate Award (to TC) and thank the University of Adelaide for the award of a M. Phil Scholarship (to RRC).

References

1. F. P. Guengerich, *Chem. Res. Toxicol.*, 2008, **21**, 70-83.
2. P. R. Ortiz de Montellano, ed., *Cytochrome P450: Structure, Mechanism, and Biochemistry* 3rd edn., Kluwer Academic/Plenum Press, New York, 2005.
3. A. Sigel, H. Sigel and R. Sigel, eds., *The Ubiquitous Roles of Cytochrome P450 Proteins*, John Wiley & Sons, Weinheim, 2007.
4. P. R. Ortiz de Montellano, *Chem. Rev.*, 2010, **110**, 932-948.
5. J. Rittle and M. T. Green, *Science*, 2010, **330**, 933-937.
6. E. M. Isin and F. P. Guengerich, *Biochim. Biophys. Acta*, 2007, **1770**, 314-329.
7. M. J. Cryle, J. E. Stok and J. J. De Voss, *Aust. J. Chem.*, 2003, **56**, 749-762.
8. S. G. Bell, N. Hoskins, C. J. C. Whitehouse and L. L. Wong, *Design and Engineering of Cytochrome P450 Systems*, 1st edn., John Wiley & Sons, 2007.
9. D. Monti, G. Ottolina, G. Carrea and S. Riva, *Chem. Rev.*, 2011, **111**, 4111-4140.
10. C. J. Whitehouse, S. G. Bell and L. L. Wong, *Chem. Soc. Rev.*, 2012, **41**, 1218-1260.
11. F. W. Larimer, P. Chain, L. Hauser, J. Lamerdin, S. Malfatti, L. Do, M. L. Land, D. A. Pelletier, J. T. Beatty, A. S. Lang, F. R. Tabita, J. L. Gibson, T. E. Hanson, C. Bobst, J. L. Torres y Torres, C. Peres, F. H. Harrison, J. Gibson and C. S. Harwood, *Nat. Biotechnol.*, 2004, **22**, 55-61.
12. S. G. Bell, N. Hoskins, F. Xu, D. Caprotti, Z. Rao and L. L. Wong, *Biochem. Biophys. Res. Commun.*, 2006, **342**, 191-196.
13. S. G. Bell, F. Xu, I. Forward, M. Bartlam, Z. Rao and L.-L. Wong, *J. Mol. Biol.*, 2008, **383**, 561-574.
14. S. G. Bell, F. Xu, E. O. Johnson, I. M. Forward, M. Bartlam, Z. Rao and L. L. Wong, *J. Biol. Inorg. Chem.*, 2010, **15**, 315-328.
15. F. Hannemann, A. Bichet, K. M. Ewen and R. Bernhardt, *Biochim. Biophys. Acta*, 2007, **1770**, 330-344.
16. F. Xu, S. G. Bell, Y. Peng, E. O. Johnson, M. Bartlam, Z. Rao and L. L. Wong, *Proteins*, 2009, **77**, 867-880.
17. S. G. Bell, A. B. Tan, E. O. Johnson and L. L. Wong, *Mol. Biosyst.*, 2010, **6**, 206-214.
18. S. G. Bell, R. Zhou, W. Yang, A. B. Tan, A. S. Gentleman, L. L. Wong and W. Zhou, *Chemistry*, 2012, **18**, 16677-16688.
19. T. Furuya and K. Kino, *Biosci. Biotechnol. Biochem.*, 2009, **73**, 2796-2799.
20. T. Furuya and K. Kino, *ChemSusChem*, 2009, **2**, 645-649.
21. T. Furuya and K. Kino, *Appl. Microbiol. Biotechnol.*, 2010, **85**, 1861-1868.
22. T. Furuya, Y. Shitashima and K. Kino, *J. Biosci. Bioeng.*, 2014.
23. S. G. Bell, W. Yang, A. B. Tan, R. Zhou, E. O. Johnson, A. Zhang, W. Zhou, Z. Rao and L. L. Wong, *Dalton Trans.*, 2012, **41**, 8703-8714.
24. P. G. M. Wuts and T. W. Greene, *Greene's Protective Groups in Organic Synthesis*, Fourth Edition edn., Wiley, 2007.
25. S. Kadkhodayan, E. D. Coulter, D. M. Maryniak, T. A. Bryson and J. H. Dawson, *J. Biol. Chem.*, 1995, **270**, 28042-28048.
26. P. J. Loida and S. G. Sligar, *Biochemistry*, 1993, **32**, 11530-11538.
27. N. Ikezawa, K. Iwasa and F. Sato, *FEBS J.*, 2007, **274**, 1019-1035.
28. M. Mizutani and F. Sato, *Arch. Biochem. Biophys.*, 2011, **507**, 194-203.
29. J. M. Fukuto, Y. Kumagai and A. K. Cho, *J. Med. Chem.*, 1991, **34**, 2871-2876.
30. K. M. Bertelsen, K. Venkatakrishnan, L. L. Von Moltke, R. S. Obach and D. J. Greenblatt, *Drug Metab. Dispos.*, 2003, **31**, 289-293.
31. K. S. Eble and J. H. Dawson, *J. Biol. Chem.*, 1984, **259**, 14389-14393.
32. K. E. Slessor, A. J. Farlow, S. M. Cavaignac, J. E. Stok and J. J. De Voss, *Arch. Biochem. Biophys.*, 2011, **507**, 154-162.

33. J. Sambrook, E. F. Fritsch and T. Maniatis, *Molecular Cloning: A Laboratory Manual*, 2nd edn., Cold Spring Harbor Laboratory Press, New York, 1989.
34. S. G. Bell, J. H. McMillan, J. A. Yorke, E. Kavanagh, E. O. Johnson and L. L. Wong, *Chem. Commun.*, 2012, **48**, 11692-11694.
35. J. W. Williams and J. F. Morrison, *Methods Enzymol.*, 1979, **63**, 437-467.
36. M. M. Chen, C. D. Snow, C. L. Vizcarra, S. L. Mayo and F. H. Arnold, *Protein Eng. Des. Sel.*, 2012, **25**, 171-178.
37. F. Xu, S. G. Bell, Z. Rao and L. L. Wong, *Protein Eng. Des. Sel.*, 2007, **20**, 473-480.
38. R. Abagyan, M. Totrov and D. Kuznetsov, *J. Comp. Chem.*, 1994, **15**, 488-506.

Table 1 Substrate binding parameters and catalytic turnover activity data for CYP199A4 with various substrates. The data are given as mean ± S.D. with $n \geq 3$. The reaction mixtures (50 mM Tris, pH 7.4) contained 0.5 μM P450, 5 μM HaPux and 0.5 μM HaPuR. Rates are given as nmol (nmol-CYP)$^{-1}$ min^{-1}.

Substrate	**% HS**	**K_d (μM)**	**N[a]**	**PFR[b]**	**Coupling (%)[c]**
4-methoxybenzoic acid	≥95%	0.28 ± 0.01	1340 ± 28	1219 ± 120	91 ± 2
2-methoxybenzoic acid	10%	n.m.[d]	-[e]	-[f]	-[f]
3-methoxybenzoic acid	40%	69 ± 2.0	498 ± 5.0	-[f]	-[f, g]
3,4-dimethoxybenzoic acid	70%	29.5 ± 3.1	807 ± 35	626 ± 100	77 ± 9
2,4-dimethoxybenzoic acid	90%	47 ± 1.0	664 ± 32	384 ± 21	58 ± 1
3,5-dimethoxybenzoic acid	10%	1500 ± 200	49 ± 2.0	7 ± 2	14 ± 4
2,5-dimethoxybenzoic acid	<10%	n.m.[d]	-[e]	-[f]	-[f]
3-hydroxy-4-methoxybenzoic acid	90%	1.7 ± 0.09	847 ± 60	663 ± 75	75 ± 8
2-hydroxy-4-methoxybenzoic acid	≥95%	0.16 ± 0.01	483 ± 32	271 ± 20	56 ± 4
6-methoxynicotinic acid	≥95%	0.46± 0.05	353 ± 6.0	286 ± 32	81 ± 8
3,4-(methylenedioxy)benzoic acid	70%	0.17 ± 0.05	265 ± 7.2	158 ± 19	59 ± 7
benzoic acid	30%	13 ± 0.2	257 ± 2.0	-[f]	-[f, h]

[a] *N*: NADH turnover rate. [b] PFR: product formation rate. [c] Coupling is the percentage of NADH consumed in the reaction that led to the formation of product arising from substrate oxidation. [d] Not reported due to low levels spin state shift preventing accurate determination (> 1.5 mM) . [e] No significant NADH oxidation activity above the leak rate. [f] no detectable levels of product formation. [g] Hydrogen peroxide levels were only 8.5 ± 1.4 μM (2.2 ± 0.7%) of the turnover. By way of comparison 4-methoxybenzoic acid turnover generated 5.5 ± 0.5 μM H_2O_2. [h] Hydrogen peroxide levels were only 18 ± 0.6 μM (4.7 ± 0.3%) of the turnover.

Figures

Scheme 1 The products formed from the CYP199A4 enzyme turnovers of the benzoic acid substrates (abbreviations; BA, benzoic acid; MBA, methoxybenzoic acid and NA, nicotinic acid).

.

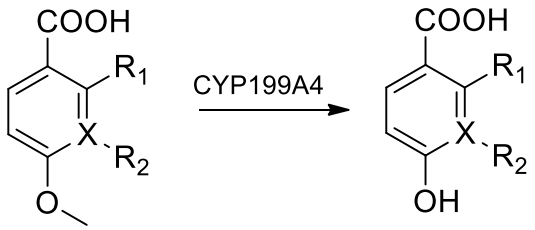

Substrate	R_1	R_2	X
4-methoxyBA	H	H	C
3,4-dimethoxyBA	H	OMe	C
2,4-dimethoxyBA	OMe	H	C
3-hydroxy-4-MBA	H	OH	C
2-hydroxy-4-MBA	OH	H	C
6-methoxyNA	H	-	N

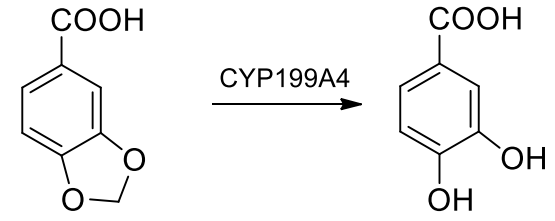

3,4-(methylene-dioxy)-benzoic acid

3,4-dihydroxy-benzoic acid

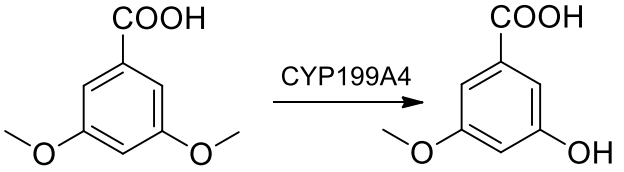

3,5-dimethoxy-benzoic acid

3-hydroxy-5-methoxy-benzoic acid

Scheme 2 The proposed mechanism of methylenedioxy ring formation catalysed by the plant P450 CYP719A family.

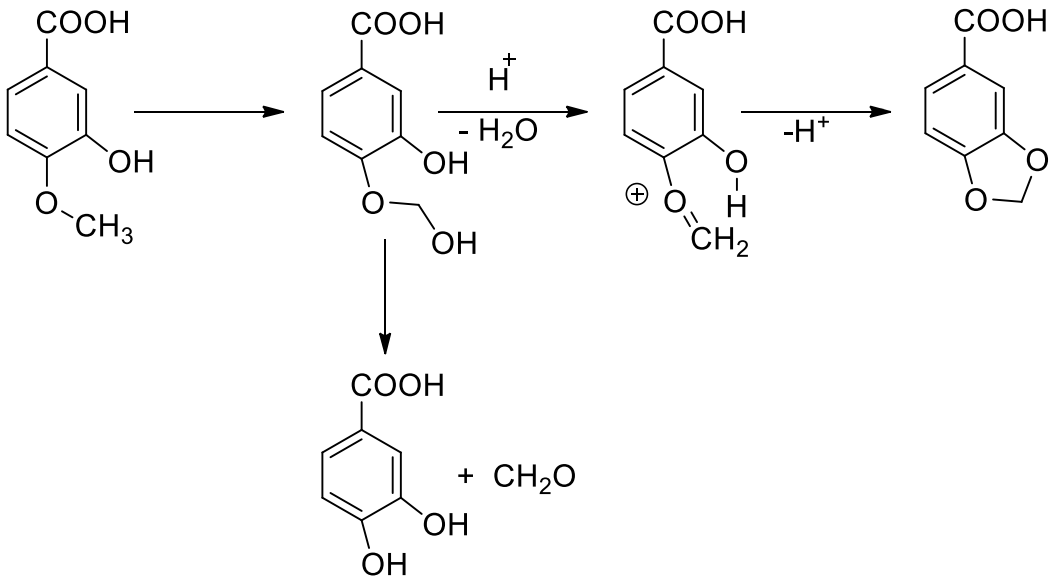

Scheme 3 Proposed reaction mechanism for methylenedioxy deprotection by mammalian P450 enzymes. Included is the proposed formation of the carbene intermediate which can act as an inhibitor of P450 enzymes by binding to the heme iron.

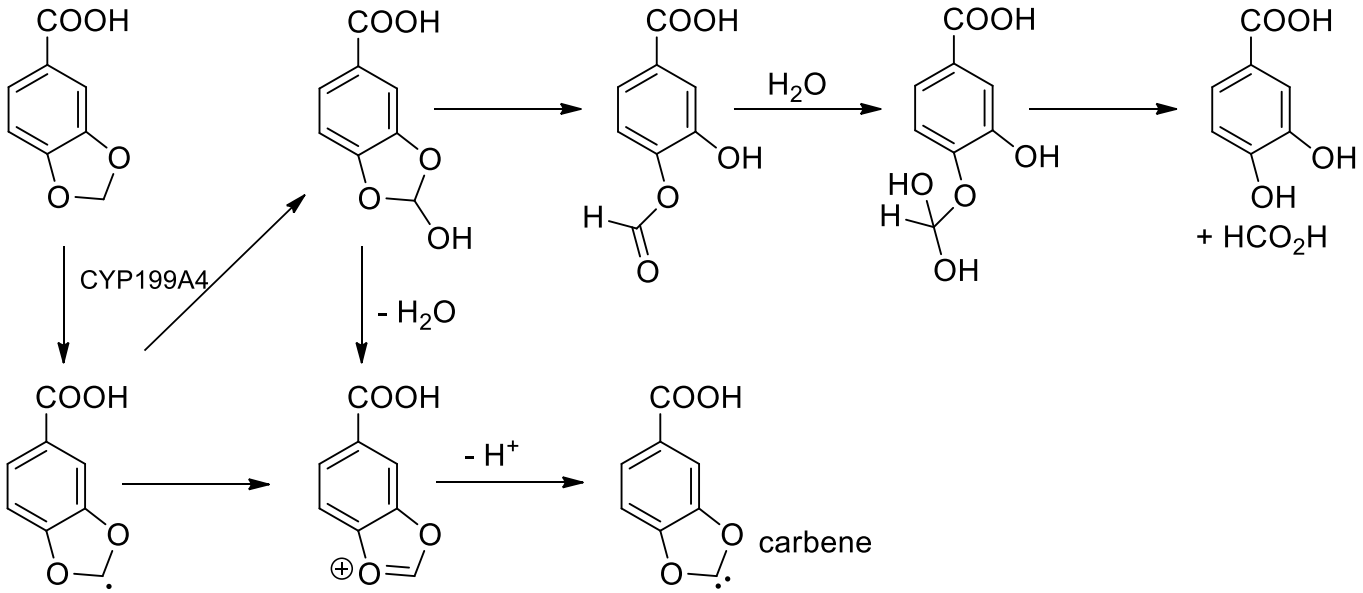

Figure 1a The substrates tested for binding and activity with CYP199A4.

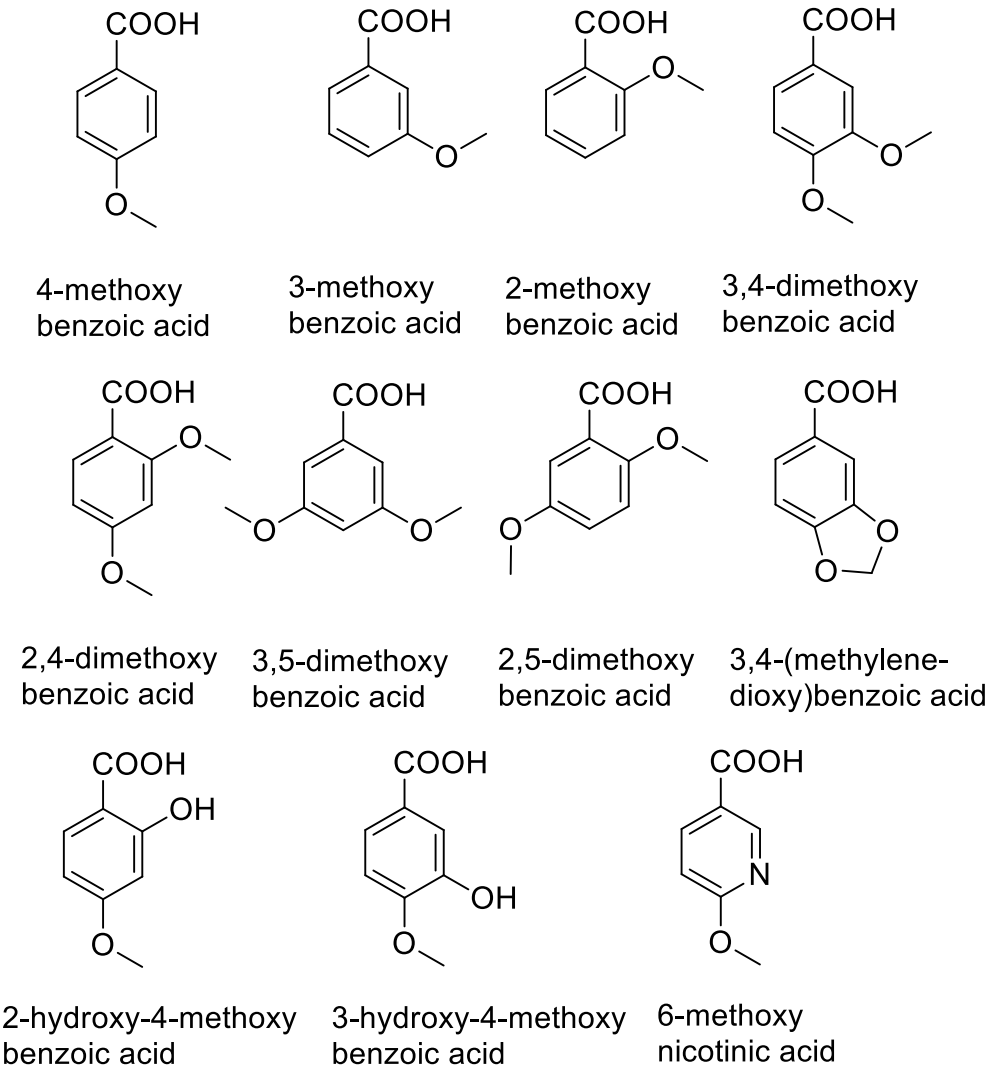

Figure 1b Spin state shift of CYP199A4 (red; substrate-bound CYP199A4, black; substrate-free CYP199A4) with the substrates (i) 3-methoxybenzoic acid (ii) 2,4-dimethoxybenzoic acid (iii) 3,4-(methylenedioxy)-benzoic acid.

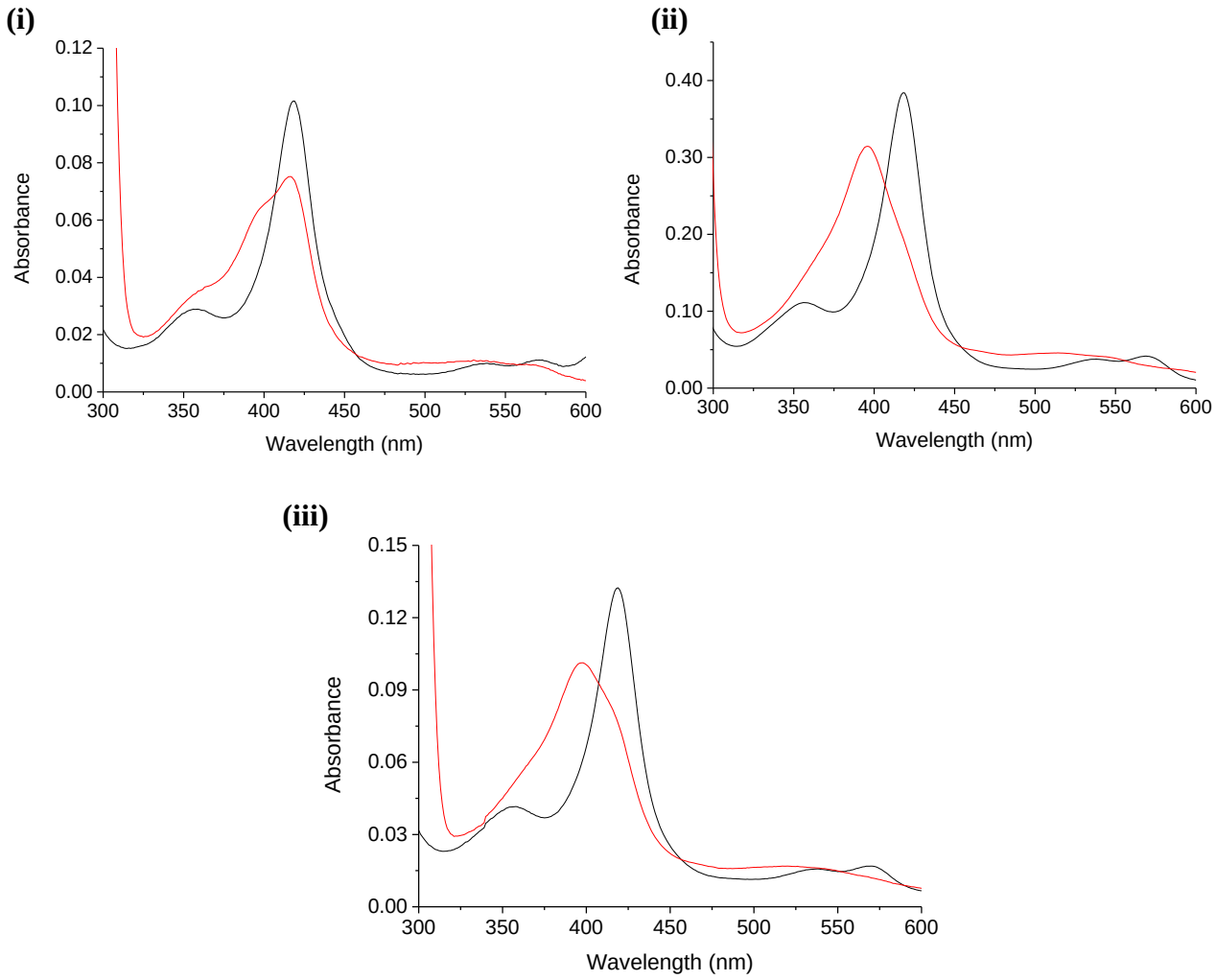

Figure 2 Dissociation constant analysis of selected substrates with CYP199A4 (a) 3-methoxybenzoic acid (b) 3,5-dimethoxybenzoic acid (c) 2-hydroxy-4-methoxybenzoic acid.

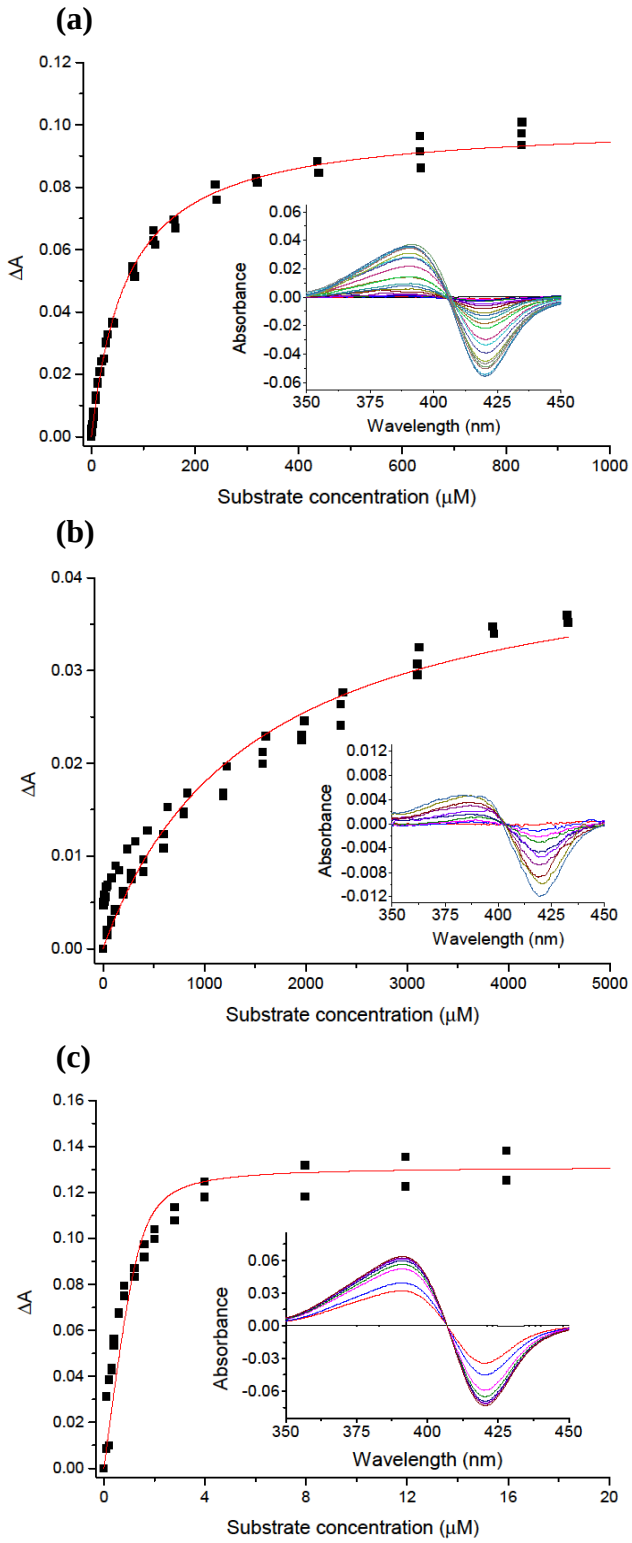

Figure 3 (a) NADH oxidation kinetic assays with 3-hydroxy-4-methoxybenzoic acid (black), 2-hydroxy-4-methoxybenzoic acid (red) and 3,4-(methylenedioxy)benzoic acid (blue). **(b)** NADH oxidation kinetic assays with 6-methoxynicotinic acid (black), 4-methoxybenzoic acid (red).

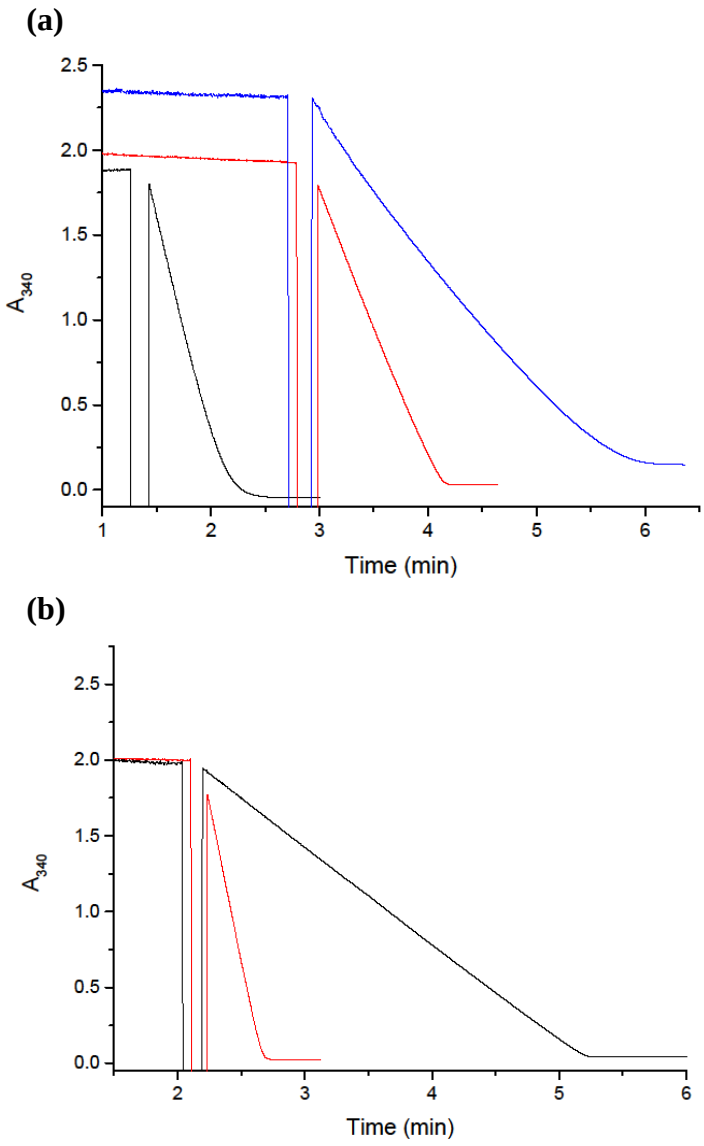

Figure 4 HPLC analysis of CYP199A4 substrate turnovers. Shown are (a) 3,5-dimethoxybenzoic acid (b) 6-methoxynicotinic acid (c) 3-hydroxy-4-methoxybenzoic acid (d) 3,4-(methylenedioxy)-benzoic acid. A gradient, 20 - 95%, of acetonitrile (with trifluoroacetic acid, 0.1%) in water (TFA, 0.1%) was used and the absorbance was monitored at 254 nm.

(a) 3,5-dimethoxybenzoic acid (turnover in black, substrate control in blue)

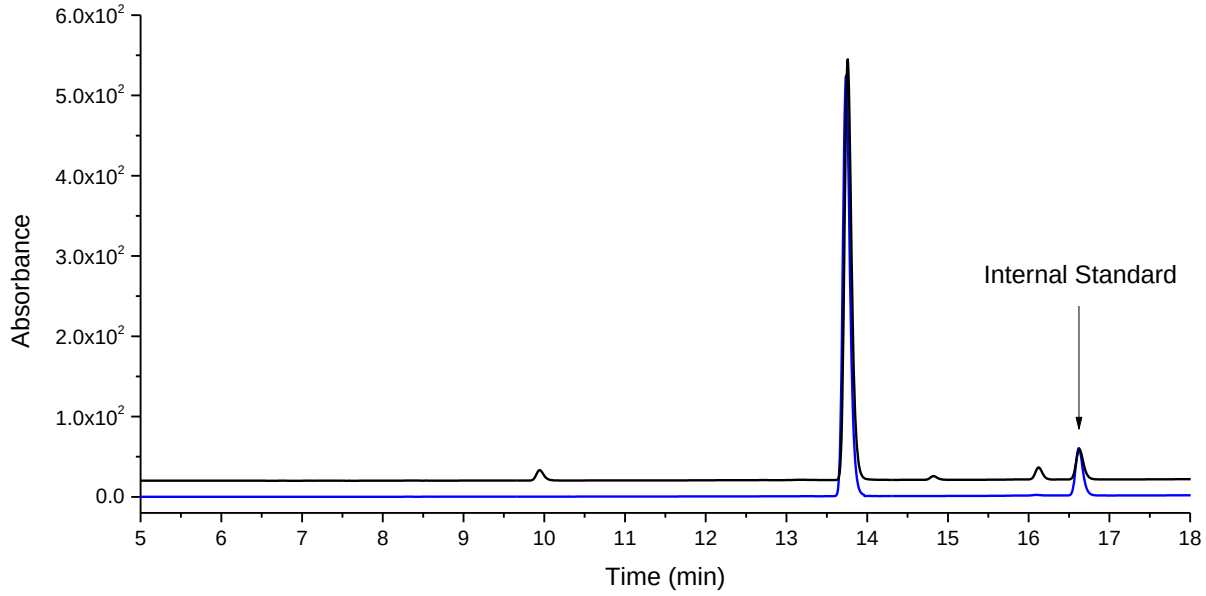

(b) 6-methoxynicotinic acid (turnover in black, substrate control in blue and 6-hydroxynicotinic acid control in red)

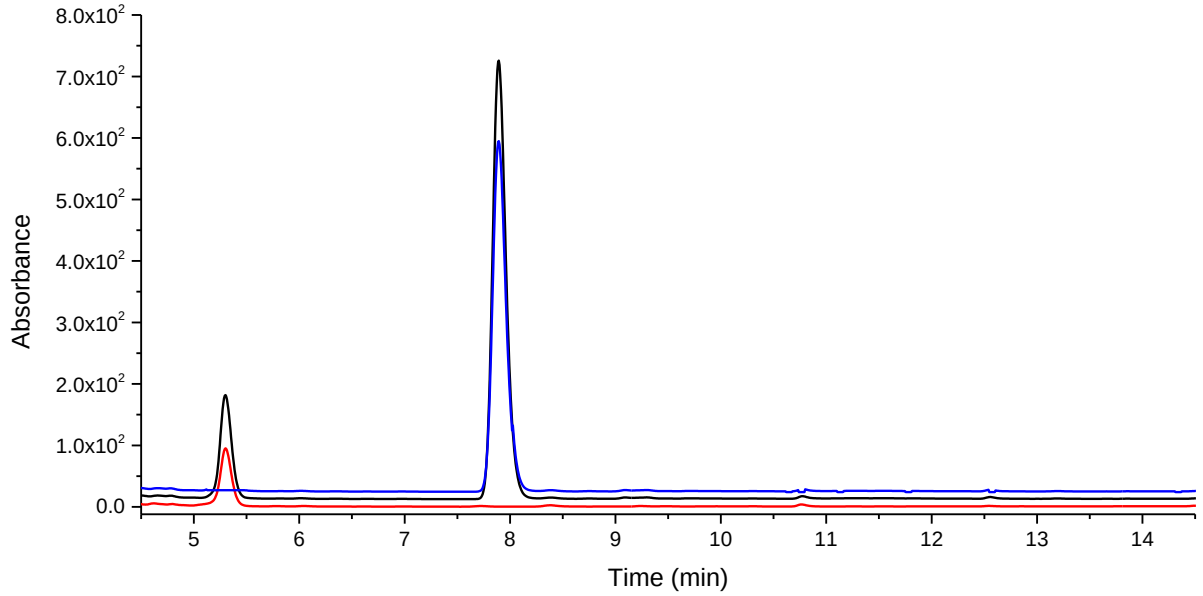

(c) 3-hydroxy-4-methoxybenzoic acid (turnover in black, substrate control in blue and 3,4-dihydroxybenzoic acid control in red)

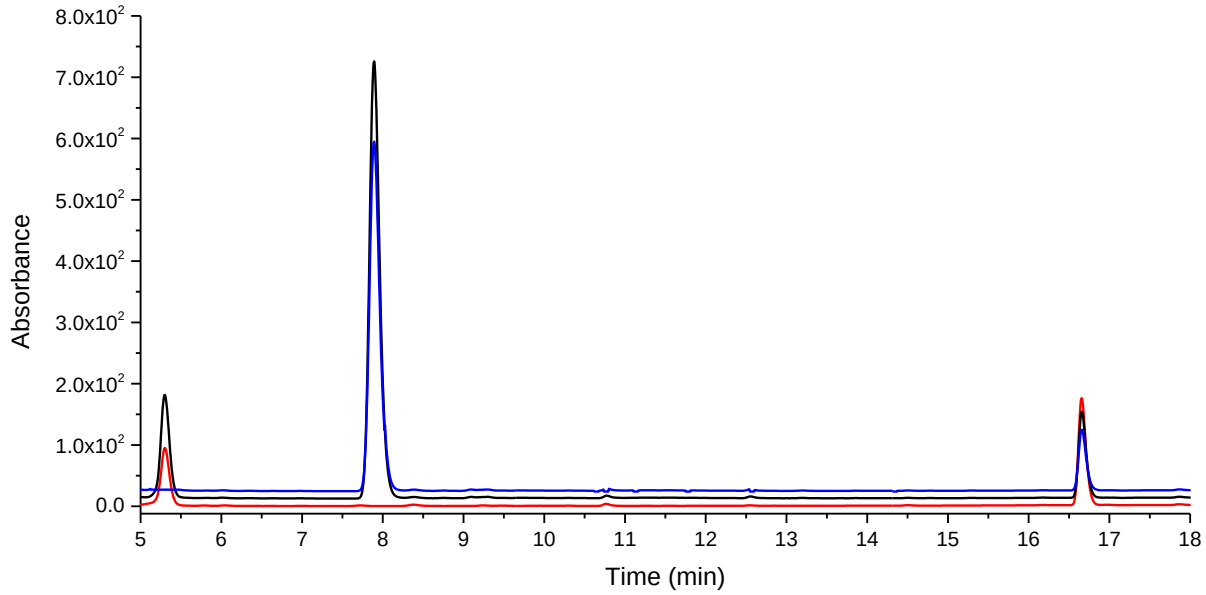

(d) 3,4-(methylenedioxy)benzoic acid (turnover in black, substrate control in blue and 3,4-dihydroxybenzoic acid control in red)

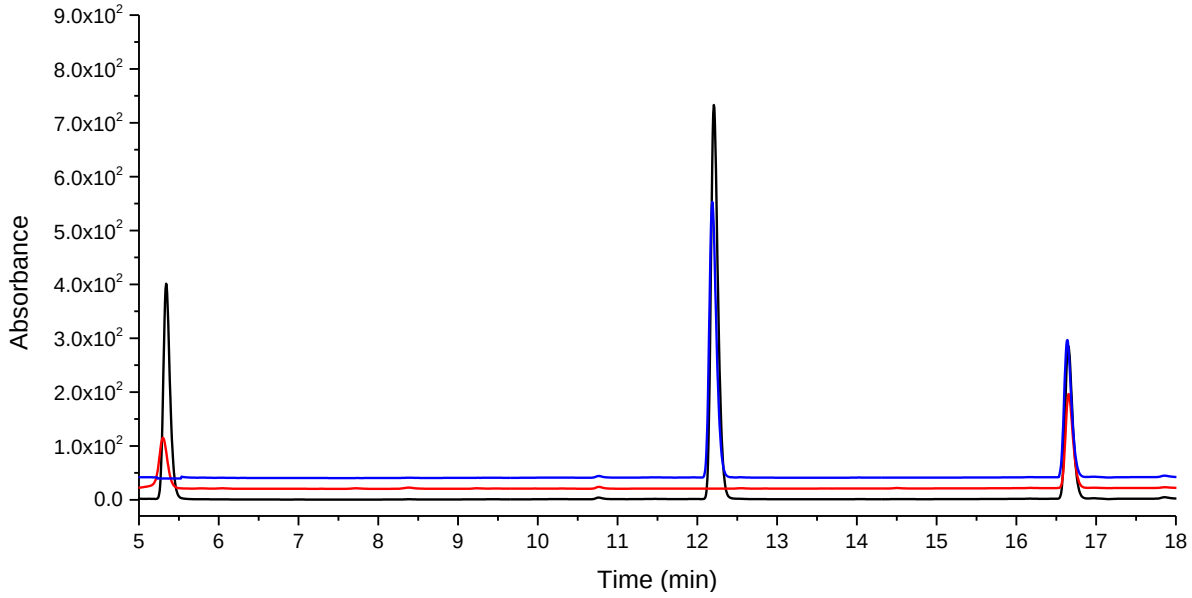

Figure 5 GC-MS analysis of CYP199A4 substrate turnovers. Shown are (a) 3,5-dimethoxybenzoic acid and (b) 2,4-dimethoxybenzoic acid and. Impurities are highlighted with an asterix.

(a)

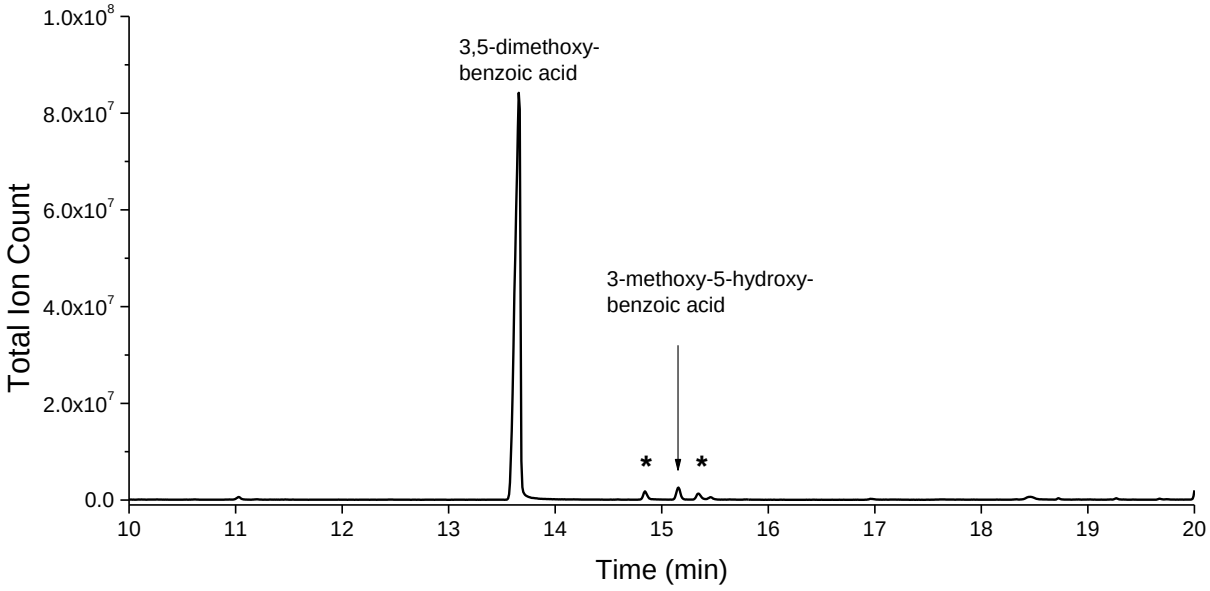

(b)

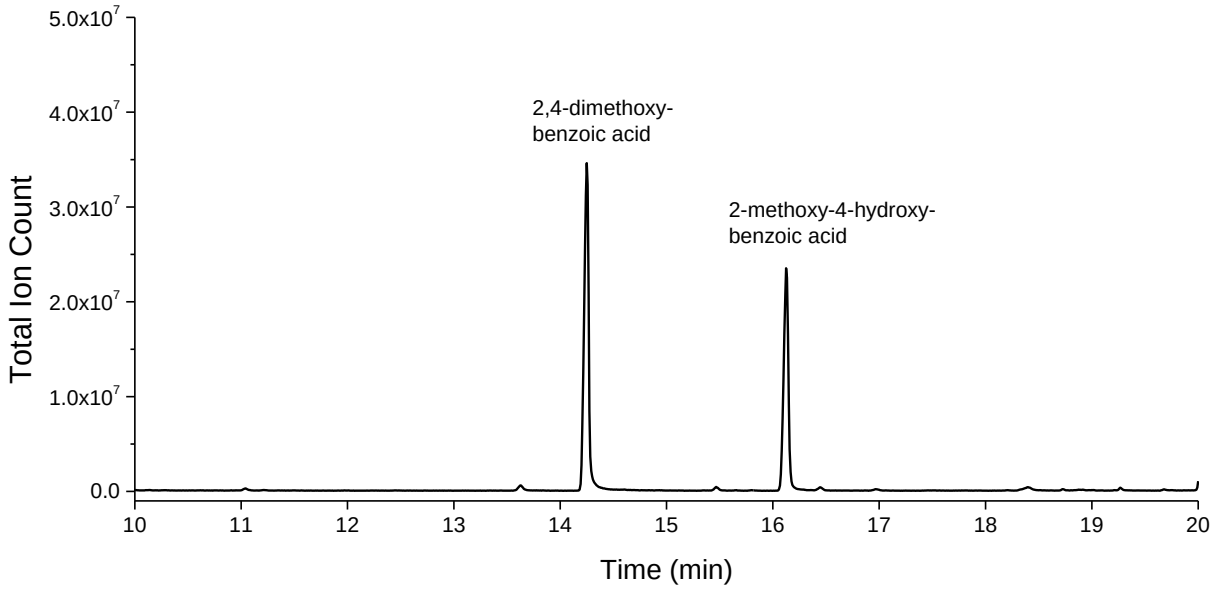

Figure 6 Structures of CYP199A4 with different substrates docked in the active site after energy minimisation. Two orientations are shown where a substitution made the substrate unsymmetrical around the C1-C4 axis. (a) 3,5-dimethoxybenzoic acid and a comparison of the orientation of 3,5-dimethoxybenzoic acid with 3,4-dimethoxybenzoic acid (PDB: 4EGN), (b) 6-methoxynicotinic acid with the pyridine nitrogen pointing towards or away from the heme and (c) 3,4-(methylenedioxy)benzoic acid and a comparison of 6-indolecarboxylic acid (PDB: 4EGO) with 3,4-(methylenedioxy)benzoic acid bound with the methylenedioxy ring orientated towards the heme. Distances are provided in the ESI as are docking studies of the other substrates (Fig. S5)

(a)

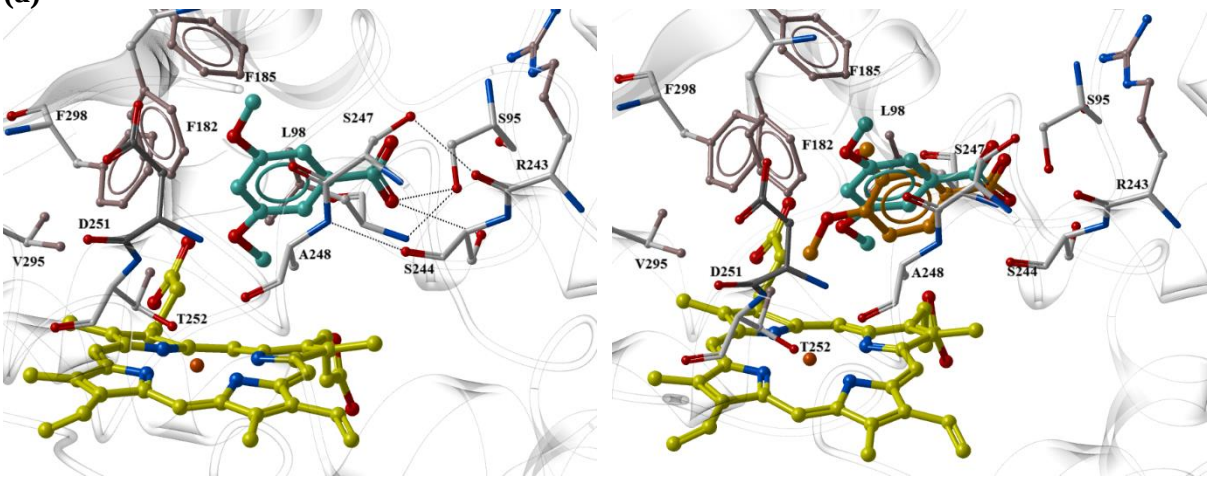

(b)

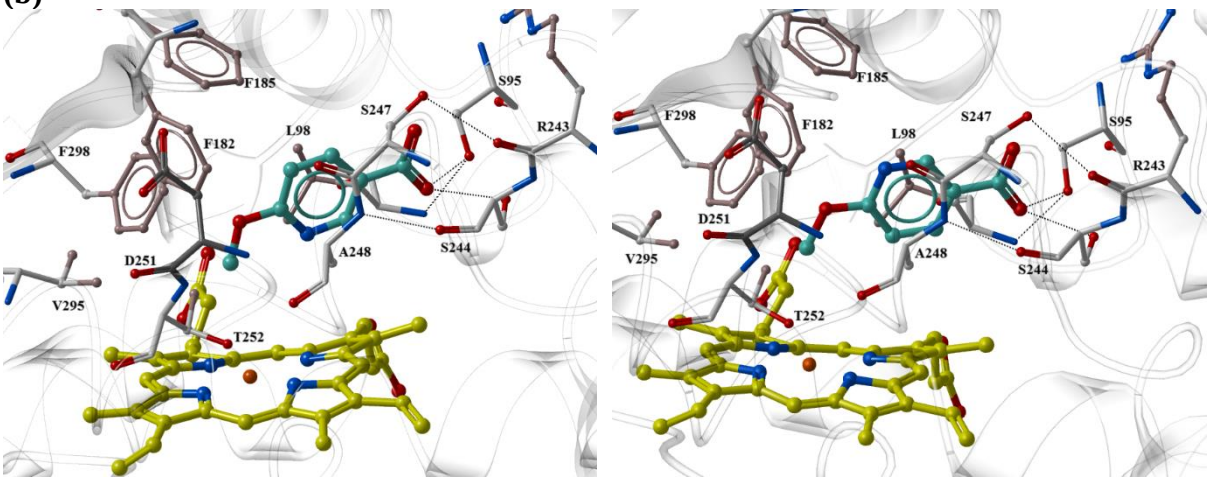

(c)

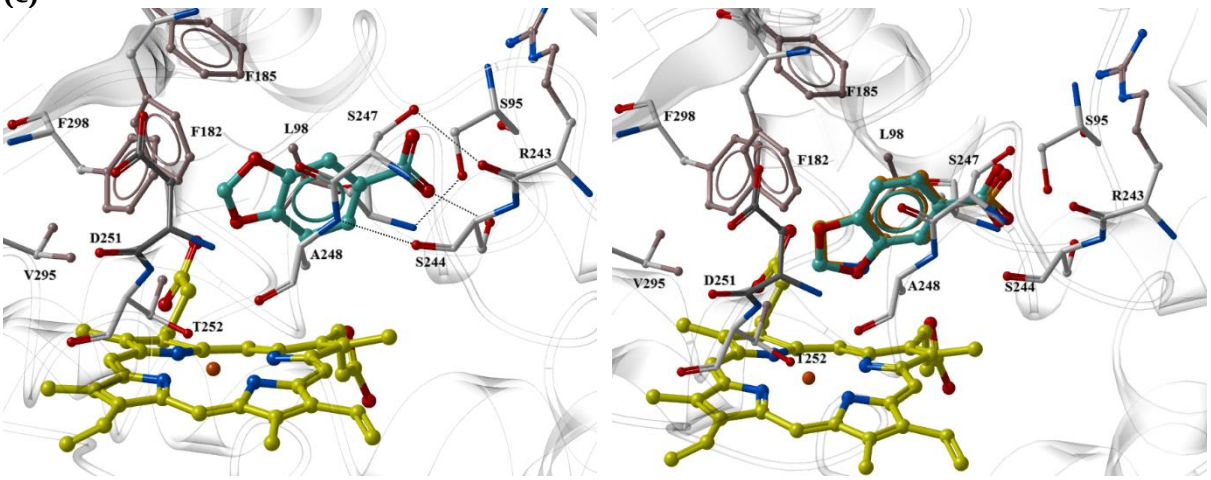

Figure 7 Purpald assay for formaldehyde formation. Black: 4-methoxybenzoic acid, red: 3,4-dimethoxybenzoic acid, blue: 3,4-(methylenedioxy)benzoic acid, pink: 3-hydroxy-4-methoxybenzoic acid. The amount of formaldehyde measured was in line with the level of product generated based on NADH added and product coupling (Table 1).